



Substantial organic impurities at the surface of synthetic ammonium sulfate particles

Junteng Wu¹, Nicolas Brun¹, Juan Miguel González-Sánchez¹, Badr R'Mili¹, Brice Temime Roussel¹, Sylvain Ravier¹, Jean-Louis Clément², Anne Monod¹

5 ¹Aix Marseille Univ, CNRS, LCE, Marseille, France

²Aix Marseille Univ, CNRS, ICR, Marseille, France

Correspondence to: Junteng Wu (junteng.wu@univ-amu.fr) and Anne Monod (anne.monod@univ-amu.fr)

Abstract

Ammonium sulfate (AS) particles are widely used for studying the physical-chemistry processes of aerosols and for instrument calibrations. Small quantities of organic matter can greatly influence the studied properties, as observed by many laboratory studies. In this work, monodisperse particles (from 200 nm to 500 nm) were generated by nebulizing various AS solutions and organic impurities were quantified relative to sulfate using a High-Resolution Time-of-Flight Aerosol Mass Spectrometer (HR-ToF-AMS). The organic content found in AS solutions was also tentatively identified using a Liquid Chromatography–tandem Mass Spectrometry (LC-MS). The results from both analytical techniques were consistent and demonstrated that the organic impurities contained oxygen, nitrogen and/or sulfur, their molecular masses ranged from m/z 69 to 420, they likely originate from the commercial AS crystals. For AS particle sizes ranging from 200 nm to 500 nm, the total mass fraction of organic (relative to sulfate) ranged from 3.8 % to 1.5 % respectively. An inorganic-organic mixture model suggested that the organic impurities were coated on the AS particle surface with a density of $1.1 \times 10^{-3} \text{ g m}^{-2}$. A series of tests were performed to remove the organic content (using pure N_2 in the flow, ultrapure water in the solutions, and very high AS quality), showing that at least 40 % of the organic impurities could be removed. In conclusion, it is recommended to use AS seeds with caution, especially when small particles are used, in terms of AS purity and water purity when aqueous solutions are used for atomization.

1 Introduction

Atmospheric aerosols are generally a complex mixture of inorganic and organic compounds that have a strong impact on climate and human health (IPCC, 2013; Pöschl and Shiraiwa, 2015). According to the annual aerosol emission inventories, inorganic compounds account for the majority of the mass (Andreae and Rosenfeld, 2008). Among them, ammonium sulfate (AS) is considered as one of the dominant components (Charlson et al., 1992; Seinfeld et al., 2016). Because AS plays important roles in physical and chemical atmospheric processes, it has been extensively used in laboratory experiments to understand and reproduce these processes. In the past 20 years, more than 200 articles have been published using AS as (seed)



30 particles for the study of optical properties, hygroscopic properties, phase transition and viscosity, as well as chemical reactivity
of aerosols (see the detailed references in SI1). In all these studies, it was shown that the presence of organic matter, even at
very low concentrations in AS particles, greatly influences these properties.

Among these, the study of aerosol hygroscopic properties represents the major contribution (115 papers out of the
263 cited in SI1). AS aerosols are very often chosen as seed particles to study hygroscopic behavior of mixed organic-inorganic
35 aerosols. Scanning various conditions of temperature and relative humidity (RH), hygroscopicity properties of aerosols were
investigated *via* measurements of hygroscopic growth, cloud condensation nuclei (CCN) activity and ice nuclei (IN) activity.
It is well acknowledged that the hygroscopic parameter kappa (κ) of pure AS particles is 0.53 [0.33 - 0.72] and 0.61 according
to the growth factor derivation and the CCN derivation, respectively (Clegg et al., 1998; Koehler et al., 2006; Petters and
Kreidenweis, 2007). Laboratory studies show that the hygroscopic behavior of most water soluble inorganic mixed aerosols is
40 additive in nature, i.e., following the ZSR (Zdanovskii, Stokes, and Robinson) assumption (Stokes and Robinson, 1966).
However, when organic compounds are present in AS aerosols, their hygroscopic properties are more complex. Firstly, for
water soluble organic compounds such as (di)carboxylic acids, their effects on AS aerosols are represented by their
hygroscopicity and mass fraction suggested by the ZSR assumption (Abbatt et al., 2005; Brooks et al., 2004; Hämeri et al.,
2002; Prenni et al., 2003). Secondly, for less soluble compounds and complex mixtures, their solubility significantly influences
45 the hygroscopic behavior of AS aerosol. At sub-saturation conditions, secondary organic aerosol (SOA) formed on AS seed
particles from α -pinene photo-oxidation lowers the hygroscopic growth factor (HGF) of AS (Meyer et al., 2009). Specifically,
at RH below the deliquescence point, AS seeded SOA do not follow the ZSR predictions due to the incomplete dissolution.
When the insoluble organic compounds are the dominant components of the aerosol, the water uptake on organic-AS particles
is significantly slowed down and requires a longer residence time to achieve the thermodynamic equilibrium (Sjogren et al.,
50 2007). The same behavior has also been observed at super-saturation conditions, i.e., the thick coating of insoluble organics
compounds such as stearic acids act as a shield preventing the interaction of AS and water, thus suppressing AS hygroscopicity
(Abbatt et al., 2005). Thirdly, several studies have observed that marine organics under low concentration and ozonolysis
products of α -pinene and monoterpene affect AS's hygroscopicity by lowering the surface tension, thus enhancing their CCN
activity (Engelhart et al., 2008; King et al., 2009; Moore et al., 2008; Wex et al., 2009). It has been shown that atmospheric
55 surfactants could reduce the aerosol surface tension by a factor of 2 compared to water surface tension (72 mN m^{-1}) (Gérard
et al., 2019; Nozière et al., 2014; Sorjamaa et al., 2004). The presence of a small amounts of surface-active organic compounds
may reduce the aerosol surface tension, affecting its hygroscopic properties: according to recent models, a reduction of 10 %
on the surface tension results in the increase of 30 % on the hygroscopic parameter κ (Ovadnevaite et al., 2017; Petters and
Kreidenweis, 2013).

60 AS has also been widely used to understand the phase transition of organic-inorganic compounds in single particles
studies (49 papers out of the 263 cited in SI1). Under sub-saturated conditions, deliquescence of pure AS occurs at ~ 80 % RH
and efflorescence at ~ 34 % RH. However, these phase transition behaviors of AS particles are significantly influenced by



organic compounds. For example, the presence of humic acids decreases the deliquescence RH and increases the efflorescence RH of AS aerosols (Badger et al., 2006). Furthermore, the presence of malonic acid on AS particle leads to a two-step deliquescence instead of a single step in the humidification process (Treuel et al., 2009). Differently to the shift of deliquescence RH and/or efflorescence RH, the presence of SOA completely removes the clear phase transition of AS on the particle: this was clearly shown for SOA derived from cycloalkene photolysis and monoterpenes photo-oxidation (Varutbangkul et al., 2006). The change in phase transition behavior of AS particle also depends on the quantity of organic compounds. In humidification process, small organic/inorganic ratios (< 20 %) lead to internally mixing and/or organic coating on the particle surface (Nandy and Dutcher, 2018; Smith et al., 2013); while high organic/inorganic ratios (> 80 %) induce liquid-liquid phase separation (Smith et al., 2013; Saukko et al., 2015).

Due to their hygroscopic properties, AS aerosols easily provide an aqueous environment, where reactions between NH_4^+ , SO_4^{2-} and water-soluble organic compounds can play an important role on the formation of secondary aerosols (62 papers among the 263 cited in SI1). Some of these reactions may explain the source of the so-called “brown carbon”, thus affecting the optical properties of particles (44 papers among the 263 cited in SI1). Ammonium cation (NH_4^+) is in pH-dependent equilibrium with dissolved ammonia in the aqueous phase. NH_3 can react with carbonyl compounds such as glyoxal, methylglyoxal, glycolaldehyde, hydroxyacetone, biacetyl or unsaturated dialdehydes in Maillard-type browning reactions to form light absorbing and oligomeric compounds such as imidazoles or pyrazine-based compounds (Hensley et al., 2021; Grace et al., 2020; Hawkins et al., 2018; Laskin et al., 2014; Kampf et al., 2012). These reactions are of particular interest for the atmosphere, as they impact on both health and climate. Their aqueous-phase processes represent an important and rapid source of brown carbon (Powelson et al., 2014; De Haan et al., 2017). In addition, SO_4^{2-} is not inert in atmospheric water. Aqueous-phase reactions with isoprene-derived epoxides to form organo-sulfates have been reported (Darer et al., 2011; Liggio et al., 2005). Epoxides, which are formed by the ozonolysis of a carbon-carbon double bond, undergo an acid-catalyzed nucleophilic attack by sulfate anions. In addition, tertiary organic nitrates, formed by nighttime NO_3^- reaction with isoprene or other terpenes, undergo nucleophilic substitution in the presence of sulfates forming organo-sulfates (Surratt et al., 2008).

Due to the atmospheric representativity of AS particles and their well-known physical and chemical properties, they are often chosen as a reference in aerosol studies, as mentioned above, and for instrumentation calibration. The presence of trace organic compounds in AS particles may induce potentially important artefacts on the experimental results of physical and chemical processes. Few laboratory studies show that organic compounds can be present in synthetic AS particles. For example, 0.8 wt % of C was observed in ammonium sulfate solutions in the study of phase transitions of AS and humic acid mixtures (Badger et al., 2006). Another example, in a study of glyoxal uptake on AS particles monitored by an Aerosol Mass Spectrometer, Trainic et al., 2011 found organic fragments on pure AS aerosols (purity not mentioned), with an organic/sulfate ratio as high as 8 %. Scanning the 263 articles (mentioned in SI1) published over the last 20 years using AS aerosols in the laboratory, it appeared that neither quantification nor identification of these potential organic impurities was reported. Furthermore, the majority of these studies (62 %) did not mention the origin and purity of AS used. As organic traces may significantly influence the properties of AS particles, and thus bias experimental results, the objectives of this work were to



quantify organic traces in commercial AS under conditions used in laboratory experiments, when possible, tentative identification was performed, and finally recommendations are given for purity improvements.

2 Method

100 AS suspended particles were generated by atomization of AS solutions at concentrations ranging from 0.01 to 0.5 M, similar to those previously employed. AS aerosols were selected at 4 sub-micrometer sizes to test the effect of particle size on the organic content. This procedure allowed to form monodisperse AS particles at mass concentrations ranging from 5 to 30 $\mu\text{g m}^{-3}$, similar to those previously employed. Their chemical composition was quantified on-line by a high-resolution time-of-flight aerosol mass spectrometer (HR-ToF-AMS). In parallel, aqueous solutions of AS were prepared and analyzed by a
105 Liquid Chromatography–tandem Mass Spectrometry (LC-MS) to tentatively identify organic content. All chemical compounds used in this work are listed in SI2.

2.1 Detection of organic traces in AS suspended particles

2.1.1 Aerosol generation and classification

A scheme of the experimental setup for quantifying organic content is shown in Figure 1. Aqueous solutions of AS
110 (0.01 - 0.5 M) were nebulized by atomization (using a TSI, 3076 atomizer) that generated droplets with compressed air at 1 bar above atmospheric pressure and a flowrate of 1.8 L min^{-1} . As a comparison with compressed air, pure N_2 (Linde Gas, 99.999 %) was used. The resulting droplets were dried by a Nafion™ dryer at relative humidity (RH) below 25 %, i.e., below the efflorescence of AS aerosol. Dry AS particles then passed through a dilution system aimed at controlling AS concentrations. It consisted in two parallel pathways, one of which was connected to a HEPA filter. An aerodynamic aerosol classifier (AAC,
115 Cambustion) and an electrostatic classifier combined with a differential mobility analyzer (DMA, TSI, 3080) were alternatively used to select monodisperse particles. The sheath/sample air flow ratio was fixed at 10 for the two classifiers. To regulate the flowrate at the exhaust, a mass flow controller (MFC) was connected to a vacuum pump. Under this configuration, the sample flow before the classifier varied from 0.4 to 1.4 L min^{-1} . This setup allowed the characterization of the suspended particles by their mobility, aerodynamic and vacuum aerodynamic sizes, as well as their organic content as a function of particle sizes with
120 respect to the total mass of AS particles selected.

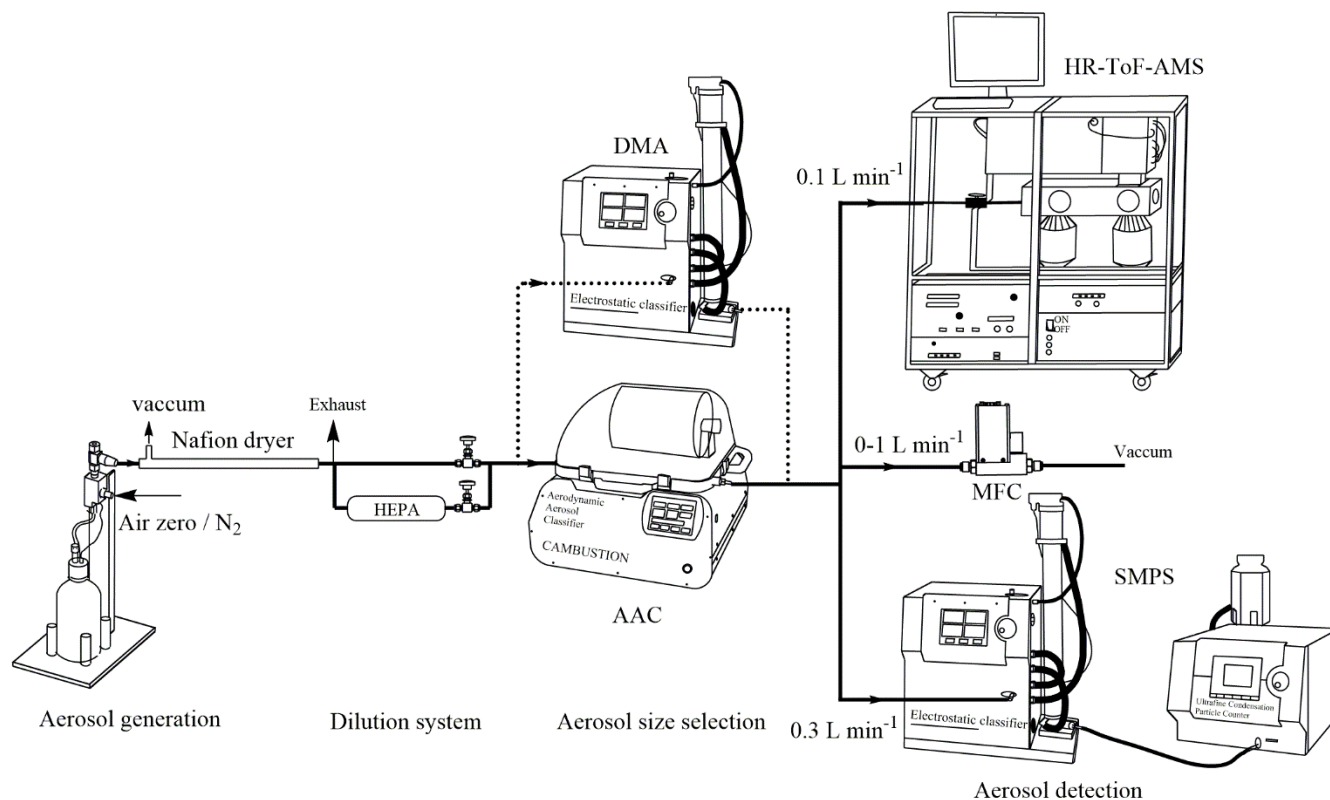


Figure 1. Experimental setup for the quantification of organic content in monodisperse ammonium sulfate particles.

2.1.2 Experimental conditions for the investigation of AS suspended particles

A series of experiments (Table 1) was performed to quantify organic content on suspended AS particles by scanning
125 various conditions of mass concentrations, particle size, and generation procedures. As organic compounds can be
homogeneously mixed in AS aerosol or remain at particle surface inducing different behavior as a function of size (Jimenez et
al., 2009; Tervahattu et al., 2002), monodisperse AS particles were selected with aerodynamic size (d_a) varied from 200 nm to
500 nm in each experiment. In experiment P1 (EXP P1), AS crystals (99.5 %, for analysis, from ACROS Organics™ Fisher
Scientific) were dissolved in Milli-Q water (18.2 MΩ cm, TOC < 2ppb) at various concentrations (0.01 - 0.5 M). In EXP P2
130 to P7, the aqueous phase concentration of AS was fixed at the highest value (0.5 M) to study the influence of other parameters.
In EXP P2, the influence of the water quality was tested. In EXP P3 to P5, the influence of the purity of AS crystals was tested.
In EXP P3, AS crystals (99.5 %, for analysis, from ACROS Organics™ Fisher Scientific) were tentatively purified by an
Accelerated Solvent Extractor (ASE 300, Dionex) using acetonitrile as extraction solvent. In EXP P4, AS crystals (99.5 %, for
analysis, from ACROS Organics™ Fisher Scientific) were tentatively purified by recrystallization in water: AS crystals (20 g)
135 were dissolved into boiling water (20 mL) reaching a concentration of 7.5 M and then recrystallized by smooth cooling at
room temperature. In EXP P5, high purity AS (99.9999% Suprapur® from Merck) was used. In EXP P6, the influence of the



particle size selector was studied by inter-comparison between the DMA and the AAC. Developed by Tavakoli and Olfert (2013), the AAC is a recent commercial aerosol classifier which selects the particle size by centrifugal force instead of electrostatic force which is used in the DMA. In the AAC, the aerodynamic diameter of selected particles is related to the rotational speed of the concentric cylinder, the sheath flow rate and the sample flow rate. Rotational speed has been reported to influence the geometric standard deviation (σ_{geo}) of size distribution, i.e., the smaller size, the higher rotational speed and the larger σ_{geo} (Johnson et al., 2018). In EXP P7, the effect of the rotational speed of the concentric cylinder in the AAC was tested while maintaining a constant size selection by regulating the MFC (Figure 1), so that the sample flow through the AAC varied from 0.4 to 1.4 L min⁻¹.

145

Table 1. Experiments to quantify organic traces on suspended AS particles under various conditions: ⁽¹⁾ AS 99.5%, for analysis, from ACROS Organics™ Fisher Scientific; ⁽²⁾ purification by solvent (acetonitrile) extraction; ⁽³⁾ purification by recrystallisation; ⁽⁴⁾ AS 99.9999% Suprapur® from Merck. ⁽⁵⁾ Milli-Q water, 18.2 MΩ cm, TOC < 2 ppb; ⁽⁶⁾ Fisher Chemical, LC-MS Grade. Under each condition, duplicate experiments were performed for each selected particle size.

Experiment	AS purity %	water	AS liquid concentration (M)	Particle size (nm)
Size selection by the AAC (sample flow = 0.4 L.min ⁻¹)				
P1	99.5 ⁽¹⁾	Milli-Q ⁽⁵⁾	0.01, 0.02, 0.05, 0.1, 0.2, 0.5	$d_a = 200, 300, 400, 500$
P2	99.5 ⁽¹⁾	Fisher ⁽⁶⁾	0.5	$d_a = 200, 300, 400, 500$
P3	99.5 ⁽¹⁾ purified ⁽²⁾	Fisher ⁽⁶⁾	0.5	$d_a = 200, 300, 400, 500$
P4	99.5 ⁽¹⁾ recryst ⁽³⁾	Fisher ⁽⁶⁾	0.5	$d_a = 200, 300, 400, 500$
P5	99.9999 ⁽⁴⁾	Fisher ⁽⁶⁾	0.5	$d_a = 200, 300, 400, 500$
Size selection by the DMA (sample flow = 0.4 L.min ⁻¹)				
P6	99.5 ⁽¹⁾	Milli-Q ⁽⁵⁾	0.5	$d_m = 122, 188, 250, 311, 375$
Size selection by the AAC (sample flow = 0.5, 1.0, 1.4 L.min ⁻¹)				
P7	99.5 ⁽¹⁾	Milli-Q ⁽⁵⁾	0.5	$d_a = 300$

150

2.1.3 Characterization of suspended particles

The particles number size distribution was measured with a scanning mobility particle sizer (SMPS) consisting of a Differential Mobility Analyzer (DMA, TSI, 3080) coupled with an Ultrafine Condensation Particle Counter (CPC, 3776, TSI). A high-resolution time-of-flight aerosol mass spectrometer (HR-ToF-AMS, Aerodyne Research) was used to measure the bulk chemical composition of non-refractory submicron particulate matter (DeCarlo et al., 2006). The instrument was used under standard conditions (vaporizer at 600 – 650 °C and electron ionization at 70 eV) in V-mode and in p-ToF mode. Each measurement point was averaged for MS cycle of 1 min and p-ToF cycle of 30 s. Calibrations with using pure and dried particles of ammonium nitrate and ammonium sulfate with a mobility diameter of 350 nm was carried out every few days of

155



operation to determine the Ionization Efficiency of nitrate, ammonium and sulfate named as IE_{NO_3} , RIE_{NH_4} and RIE_{SO_4} . The
160 RIE_{NH_4} and RIE_{SO_4} values obtained experimentally are 3.3 and 1.8, respectively. The standard recommended value for RIE_{org}
of 1.4 was used for organics. Calibration in p-ToF mode was carried out using pure ammonium nitrate in the size range 80-
500 nm mobility diameter. The data treatment has been performed by AMS Analysis Toolkit 1.63 and PIKA 1.23 under the
software Igor Pro 6.37. The selection of ions to fit in PIKA was derived from the mass spectra produced by AS aerosols at d_a
= 200 nm in EXP P1 and was re-checked in each experiment. The measured mass spectra were dominated by NH_x and SO_x
165 fragments, but air fragments such as N^+ , O^+ , HO^+ , H_2O^+ , N_2^+ , $^{15}NN^+$, O_2^+ , $^{18}OO^+$, Ar^+ , CO_2^+ showed also large ion signals. To
avoid any over-estimation of the organic fraction, only CHO^+ and CO_2^+ were apportioned to organics using $C_2H_3O^+$ following
the procedure of Aiken et al., (2007) and Canagaratna et al., (2015).

2.2 Seeking for organic traces in AS aqueous solutions

In parallel with the characterization of suspended AS particles, organic traces were investigated directly in AS
170 aqueous solutions by Liquid Chromatography–tandem Mass Spectrometry (LC-MS) for tentative molecular identification. The
system comprised liquid chromatography (Acquity system, Waters) coupled with Quadrupole-Time-of-Flight Mass
Spectrometry (Synapt G2 HDMS, Waters) fitted with an electrospray ion source (ESI). The chromatographic separation was
carried out on an Atlantis T3 reversed phase C18 column (100*2.1; 3 μm , Waters), the mobile phase consisted in two eluents:
eluent A was Milli-Q water (resistivity 18 $M\Omega\ cm^{-1}$ at 25 °C) with 0.1 % formic acid, and eluent B was either methanol
175 (Optima[®] LC/MS grade, Fisher Scientific) with 0.1 % formic acid or acetonitrile (Fisher Chemical, Optima[®] LC/MS grade)
with 0.1 % acid. The gradient elution was performed at a flow rate of 0.4 $mL\ min^{-1}$ using 5 % of (B) held 1 min and 5 – 95 %
of (B) within 5 min. The sample injection volume was 5 μL . In the ESI, the capillary voltage was set to 1 kV, the desolvation
gas flow was 1000 $L\ h^{-1}$ at 500 °C and the source temperature was 150 °C. During each chromatographic run, leucine
enkephalin (2 $ng\ \mu L^{-1}$, $C_{28}H_{37}N_5O_7$, molecular weight 555.27 $g\ mol^{-1}$, Sigma-Aldrich) was used as internal standard to perform
180 mass correction. The mass spectrometer was tuned to V-mode with a resolving power of 18 000 at m/z 400 and allowed the
determination of elemental composition with a mass accuracy lower than 5 ppm. For elemental attribution, the ranges of atom
number were set as follows: C [0-30], H [0-60], N [0-5], O [0-10], S [0-3], P [0-3], Na [0-1] thus covering the most common
elements (Kind and Fiehn, 2007). An isotope prediction algorithm, based on the mass of the molecular ion and the relative
intensity of the 1st and 2nd isotopes, was applied to reduce the number of proposed elemental compositions. Data were collected
185 from 50 to 600 Da in the positive and negative ionization modes. All products were detected as their protonated molecules
($[M+H]^+$) or sodium adducts ($[M+Na]^+$) in the positive mode, and their deprotonated molecules ($[M-H]^-$) in the negative mode.
In some experiments, complementary analyses were performed using MS/MS fragmentation with various collision energies.

Although the organic purity is not mentioned on commercial crystals (only the inorganic content is indicated), two
different brands of AS of the same purity were analyzed to seek for potential organic traces and for comparison purposes: one
190 from ACROS Organics[™] Fisher Scientific (99.5 %, for analysis) that has been widely used in the literature and one EMSURE[®]



from Merck (99.5 %, for analysis). The characterization experiments are shown in Table 2, each one was systematically complemented by blank experiments, i.e., analysis of the water used for each AS solution.

195 Table 2: Experiments of characterization of organic traces in AS liquid solutions. The elution gradient and ESI setup were the same for all experiments. ⁽¹⁾ AS 99.5%, for analysis, from ACROS Organics™ Fisher Scientific; ⁽²⁾ AS 99.5% EMSURE® from MERCK ⁽³⁾ Eluents: A= H₂O with 0.1% formic acid, and B as specified; ⁽⁴⁾ acetonitrile, ⁽⁵⁾ methanol, ⁽⁶⁾ methyl tert-butyl ether, ⁽⁷⁾ dichloromethane. L-L: liquid-liquid, S-L: solid-liquid.

Experiment	Type of experiment				LC-MS analytical conditions	
	AS purity %	AS aqueous concentration	Sample preparation	Extracting solvent	Eluent B ⁽³⁾	MS Mode
C1	99.5 ⁽¹⁾	1.5 M	No (direct injection)	-	ACN ⁽⁴⁾ 0.1% acid	ESI ⁺ -MS
C2					MeOH ⁽⁵⁾ 0.1% acid	
C3			L-L extraction	MTBE ⁽⁶⁾	ACN ⁽⁴⁾ 0.1% acid	ESI ⁺ -MS / ESI-MS
C4				DCM ⁽⁷⁾		
C5		S-L extraction	ACN ⁽⁴⁾	MeOH ⁽⁵⁾ 0.1% acid		
C6					2.5 M	
C7		crystals	L-L extraction	ACN ⁽⁴⁾	MeOH ⁽⁵⁾ 0.1% acid	ESI ⁺ -MS-MS
C8						
C9	99.5 ⁽¹⁾	5 M	L-L extraction	ACN ⁽⁴⁾	MeOH ⁽⁵⁾ 0.1% acid	ESI ⁺ -MS / ESI-MS
C10	99.5 ⁽²⁾	5 M	L-L extraction			

200 In EXP C1 and C2, aqueous solutions of AS were directly injected into the LC-MS, and two elution solvents were tested to optimize the chromatographic separation, the signal was only monitored in ESI⁺. In EXP C3 to C10, organic compounds were extracted from AS crystals by different methods (solid-liquid and liquid-liquid extraction) using various solvents, and preconcentrated prior LC-MS analysis using both positive and negative modes. For these extractions, an Accelerated Solvent Extractor (ASE 300, Dionex) system was used under the following conditions: acetonitrile was the extraction solvent, the oven was set at 100 °C under 100 bars, the heat up time and static time were 5 min each, three extraction
 205 cycles were operated. As an extension of EXP C6, EXP C9 was designed to perform MS/MS analysis using very high

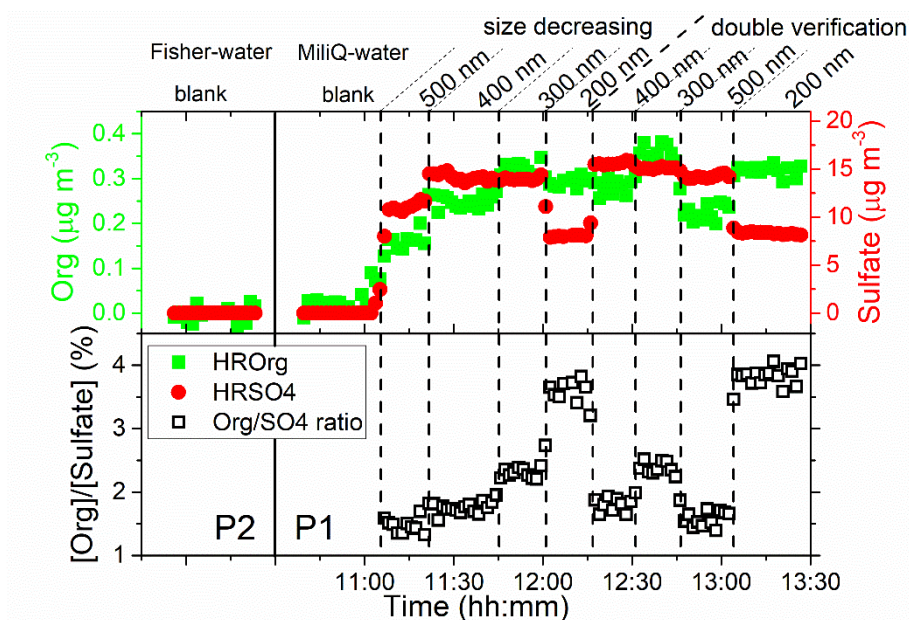


concentrations of AS to optimize the identification of organic traces, and analysis were performed in the positive mode only. For comparison purposes, another brand of AS of the same purity (99.5 %) were used in EXP C8 and C10 using two extraction methods.

3 Results and discussions

210 3.1 Organic content on AS suspended particles

A significant quantity of organic matter was directly observed by the HR-ToF-AMS in EXP P1. As an example, Figure 2 shows the mass concentrations of total organic matter and sulfate and their ratios as a function of time during one size cycle performed in EXP P1 at AS concentration of 0.01 M. Figure 2 also provides background signals obtained with the two pure waters in different qualities used in EXP P1 and P2. In these background signals, the total mass concentrations of organics and sulfate are $0.018 \pm 0.009 \mu\text{g m}^{-3}$ and $0.002 \pm 0.001 \mu\text{g m}^{-3}$ respectively, similar to the detection limits of the HR-ToF-AMS in the V mode (DeCarlo et al., 2006). In the presence of AS, a significant quantity of organics was observed with concentrations ranging from 0.15 to $0.33 \mu\text{g m}^{-3}$ when aerodynamic size of the particle varied from 500 nm to 200 nm, with a very good reproducibility in the duplicate experiments, at each size. Furthermore, the evolution of the mass ratio between total organic and sulfate marked as [Org]/[Sulfate] (Fig. 2) shows a clear correlation with particle size: this ratio increases when the particle size decreases. The same observations were made at all other AS concentrations investigated in EXP P1 and in the other experiments. Overall, it was observed that [Org]/[Sulfate] varied from 1.5 % to 3.8 %, slightly higher (respectively lower) than in the two previous studies mentioning the presence of organic in laboratory experiments on AS particles (respectively Badger et al., 2006 and Trainic et al., 2011).



225

Figure 2: Mass concentrations of total organic matter, sulfate and organic/sulfate ratio as a function of time during one cycle performed in EXP P1 at AS concentration of 0.01 M. Background signal obtained with pure water in EXP P1 and P2 is also shown for quality check and for comparison between the two pure waters in different qualities.

The total mass concentration of organic compounds was calculated based on all organic fragments, as described in the previous Sect 2.1.3. Figure 4 shows the Unit-mass HR-ToF-AMS spectrum of AS aerosols selected by the AAC at $d_a = 200$ nm.

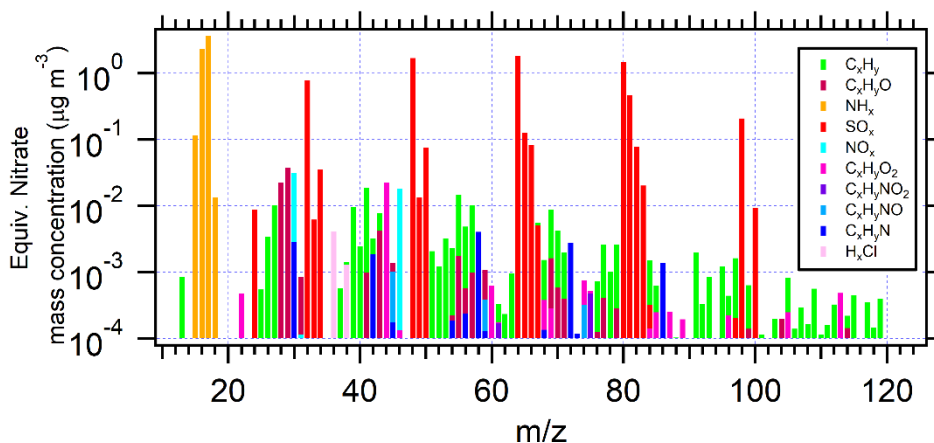


Figure 3 : Unit-mass spectra (averaged over 12 measurement runs) of AS suspended particles ($d_a = 200$ nm) in EXP P1, performed at AS concentration of 0.5 M.

235

Representing sulfate and ammonium respectively, SO_x^+ and NH_x^+ are the major fragments. All the other fragments are between 1 and 3 orders of magnitude lower, but detectable signals span for m/z up to 100. The low signal detected for the



NO⁺ and NO₂⁺ fragments at m/z 30 and 46, inhibits the distinction between inorganic and organic nitrate. Concerning organic fragments, significant signals were observed for fragments C_xH_y⁺ at m/z 27, 39, 41, 43, 55, 57, 67, 69, for C_xH_yO⁺ at m/z of 28 and 30, for C_xH_yO₂⁺ at m/z 44, for C_xH_yN⁺ at m/z 30, 58, 72, 86 (raw spectra of CHN fragments are shown in SI3). These signals seem to represent large organic molecules bearing various functionalities, potentially comprising oxygen and nitrogen. Before further identification of these compounds, Sect 3.2 and Sect 3.3 present the results and discussions on the influence of the particle size and liquid AS concentrations on the organic content.

3.2 The role of particle size and liquid AS concentrations on the quantity of organic content

Figure 4 shows the [Org]/[Sulfate] measured in AS aerosols at various nebulized solution concentrations as a function of particle size. While no significant influence of AS aqueous phase concentration has been found (within experimental uncertainty), a significant influence of particle size is clearly observed on the [Org]/[Sulfate].

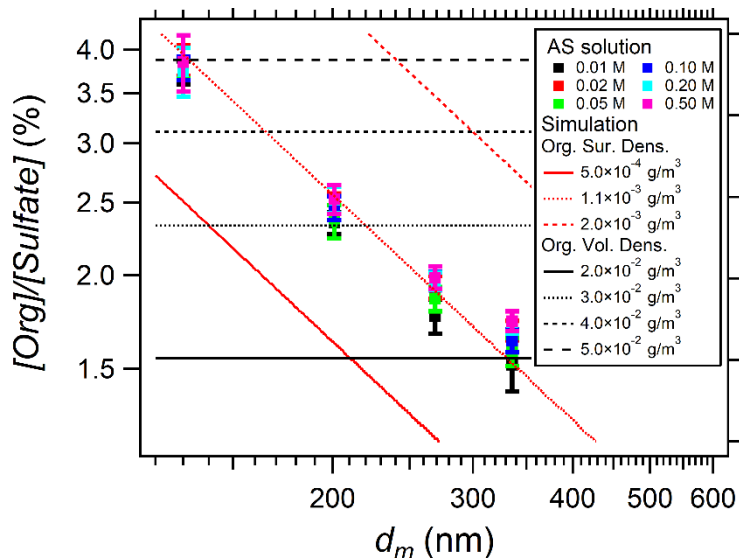


Figure 4 : Organic/sulfate mass concentration ratios in AS aerosols versus particle mobility size (d_m) during EXP P1 scanning the six nebulized AS concentrations (0.01 to 0.5 M). The colored dots (with error bars) are the experimental data, while the red and black lines represent the calculated [Org]/[Sulfate] considering either surface coating of organic matter (in red from Eq. 3) or internal mixing (in black from Eq. 4)

To further understand how the organic matter was mixed with AS aerosols, two series of calculations were performed, following two hypothesizes on the organic-inorganic mixing: i) organic coating on the surface of monodisperse AS particles, and ii) internal mixing. To achieve this calculation, a thorough study of the morphology of AS particles was needed which was obtained from multi-characterization of particle size. For monodisperse AS particles selected by the AAC at a required aerodynamic diameter (d_a), its mobility diameter (d_m) and vacuum aerodynamic diameter (d_{va}) were measured by SMPS and HR-ToF-AMS, respectively.

The calculations performed under each of the two hypothesizes on the organic-inorganic mixing are detailed hereafter:



- Hypothesis 1: AS aerosols were coated by organic compounds with a size-independent density $\rho_{org,S}$ (in g m^{-2}).

260 For non-spherical particle, the total surface of particle was considered as the surface of volume equivalent particle. According to DeCarlo et al., (2004), the relation between volume equivalent diameter (d_{ve}) and d_a is determined in Appendix A.

$$d_a = d_{ve} \sqrt{\frac{\rho_p}{\rho_0} \frac{1}{\chi} \frac{C_c(d_{ve})}{C_c(d_a)}} \quad (1)$$

Where χ is the shape factor of aerosol particles and C_c is the Cunningham slip factor (Kim et al., 2005), given by Eq. 2.

$$C_c(K_n) = 1 + K_n \left[1.165 + 0.483 \exp\left(-\frac{0.997}{K_n}\right) \right] \quad (2)$$

265 $K_n(d) = 2\lambda_g/d$ is the Knudsen number, and λ_g is the gas mean free path. In this work, normal temperature and pressure (293.15 K at 1 atm) were applied for the calculation of the shape factor of AS aerosols. In this work, morphological properties of AS particles are shown in Appendix A: Morphological properties of AS aerosols. Therefore, the prediction of surface coated organic compounds compared to sulfate mass is described in Eq. 3.

$$\frac{[Org]}{[Sulfate]} = \frac{\rho_{org,S} S_{ve}}{V_{ve} \rho_{AS} \frac{M_{SO_4}}{M_{AS}}} = \frac{3}{2} \frac{\rho_{org,S}}{d_{ve} \rho_{AS} \frac{M_{SO_4}}{M_{AS}}} \times 100\% \quad (3)$$

270 Where S_{ve} and V_{ve} are respectively the surface and volume of the volume equivalent AS particle. [Org] and [Sulfate] are the mass concentrations of organic compounds and of sulfate in the particulate phase. Eq. 3 shows that, in this case, the ratio [Org]/[Sulfate] decreases when the particle size increases.

- Hypothesis 2: Organic compounds are homogeneously mixed in AS aerosols with an density $\rho_{org,V}$ (in g/m^3). In this case, the mass concentrations of organic compounds compared to sulfate is described by Eq. 4.

$$\frac{[Org]}{[Sulfate]} = \frac{\rho_{org,V} V}{V \rho_{AS} \frac{M_{SO_4}}{M_{AS}}} = \frac{\rho_{N,intern}}{\rho_{AS} \frac{M_{SO_4}}{M_{AS}}} \times 100\% \quad (4)$$

275 Where V is the total volume of studied aerosol particle. In this case, the ratio [Org]/[Sulfate] is independent to particle size.

The results of these two calculations are shown in Fig. 4 together with the experimental results. The comparison clearly shows that the organic compounds coat homogeneously on the surface of AS particles with a surface density of $1.1 \times 10^{-3} \text{ g m}^{-2}$. In addition, this result also shows that the Nafion™ dryer is not efficient in removing these organic
280 compounds, probably due to their low volatility.

3.3 Influence of AAC and DMA on the organic content

Particle size selection is important in aerosol science especially when particle size influences the properties studied. In this work, both AAC and DMA were used to provide monodisperse AS aerosols. As a recent commercial instrument, AAC was used to select AS aerosols in most of the experiments. The effects of the concentric cylinder rotation speed of the AAC were tested in EXP P7. The results (SI4) demonstrate that the rotation speed does not affect the $[\text{Org}]/[\text{Sulfate}]$. While the AAC selects particles using centrifugal force, the DMA selects particles bearing a given electrical mobility size, providing size distributions that are not perfectly monodisperse but with double or triple modes, due to multi-charging effects. DMA has been widely used so corrections of these effects have been successfully applied in aerosol studies (Petters, 2018; Wiedensohler et al., 2012). In this work, we compared $[\text{Org}]/[\text{Sulfate}]$ in AS particles selected by the DMA and by the AAC respectively (Figure 5).

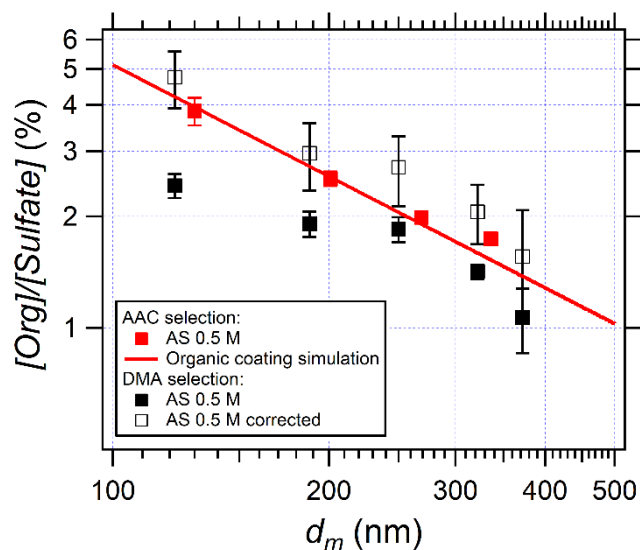


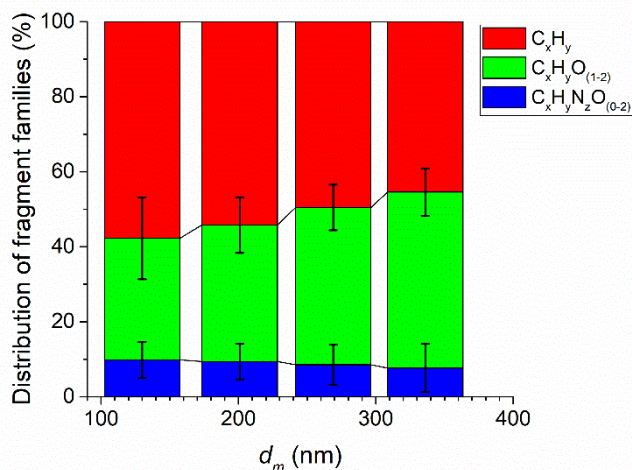
Figure 5 : Influence of instrumental conditions and instrument inter-comparison: AAC selection (red squares, EXP P1), DMA selection (black squares, EXP P6) and multi-charging correction (white squares). The red line represents the calculation simulating organic coated at the AS particle surface using Eq. 3 with a surface density of $1.1 \times 10^{-3} \text{ g m}^{-2}$ (selected from Fig. 4).

The white squares represent the multi-charging corrections considering the hypothesis that organic compounds coat the surface of AS particles as shown in Sect 3.2. Details of the multi-charging corrections are given in SI5. Briefly, the corrected $[\text{Org}]/[\text{Sulfate}]$ by the multi-charged modes are systematically higher than the non-corrected values because the correction considers the total amounts of organics and sulfate. From the results, using the DMA selection after correction, the $[\text{Org}]/[\text{Sulfate}]$ is clearly inversely related to the mobility size and in very good agreement with those obtained using the AAC selection. In conclusion, the intercomparison of the two instruments shows that the influence of the instrument is negligible, and it also shows that the selection by AAC leads to lower uncertainties and therefore more accurate results.



3.4 Tentative Identification of organic content

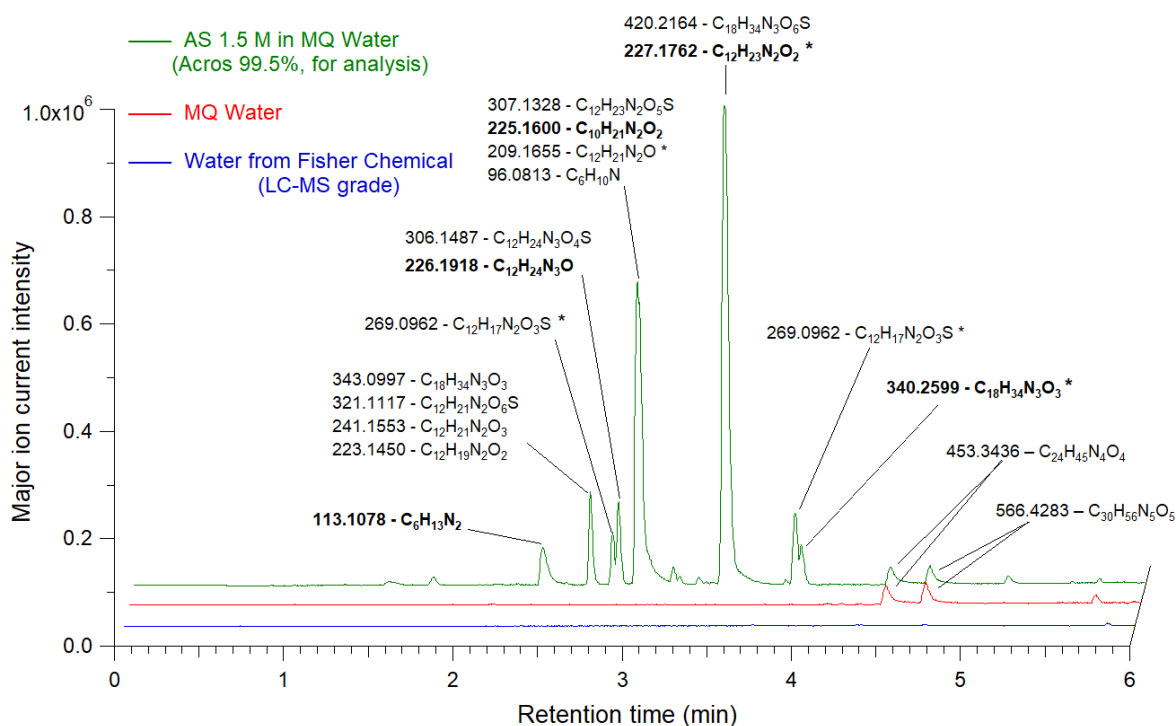
From the HR-ToF-AMS mass spectra, the three main organic fragments present in AS particles were C_xH_y , $C_xH_yO_{(1-2)}$ and $C_xH_yNO_{(0-2)}$. Figure 6 shows the proportion of these three groups relative to total organics as a function of AS particle size. Within the uncertainties, the proportion of the three families remains constant and independent on the particle size, which shows the stability of the organic compounds coated on AS particles.



310 **Figure 6:** Mass fractions of the three main sets of organic fragments present in AS particles as measured by the HR-ToF-AMS during EXP P1.

The identification of the corresponding organic compounds was limited by the high fragmentation due to the electron impact ionization operated in the HR-ToF-AMS instrument. Further identification was investigated LC-MS on liquid AS solutions. In EXP C1 and C2, an aqueous solution of ammonium sulfate (99.5 %) at 1.5 M was directly injected and was analyzed in the positive mode. Figure 7 shows a chromatogram of this ammonium sulfate solution (green line) as well as blanks of Milli-Q water (red line) and Fisher water (blue line). In Milli-Q water, two ions were present at retention times 4.45 min and 4.65 min, their mass spectra were attributed as nylon polymers $(C_6H_{11}NO)_n$ which are among the frequently reported interfering compounds (Tran and Doucette, 2006; Keller et al., 2008). However, no significant contamination was observed in the Fisher water (LC-MS Grade). Figure 7 shows that the same ions found in Milli-Q water were also present in the AS solution prepared in the same Milli-Q water. Many other ions were detected in the AS solution, and their retention times highly suggested that these molecules were organic. The proposed raw formulas systematically contained carbon, hydrogen, oxygen, nitrogen and sometimes sulfur, consistent with the HR-ToF-AMS spectra. The double bond equivalence varies from 1.5 to 5.5 showing that the molecules are unsaturated and potentially cyclic. Different to nylon polymers found in Milli-Q water, these raw formula are not referenced among the common laboratory LC-MS contaminants (Keller et al., 2008). The mass error was always well below 5 ppm and no raw formula with sodium adduct was suggested that most intense ions detected in the AS

solution are described in more details in SI6, where some of the m/z show two different retention times implying potentially the presence of isomers, for example at m/z 225.1600 and 226.1918.



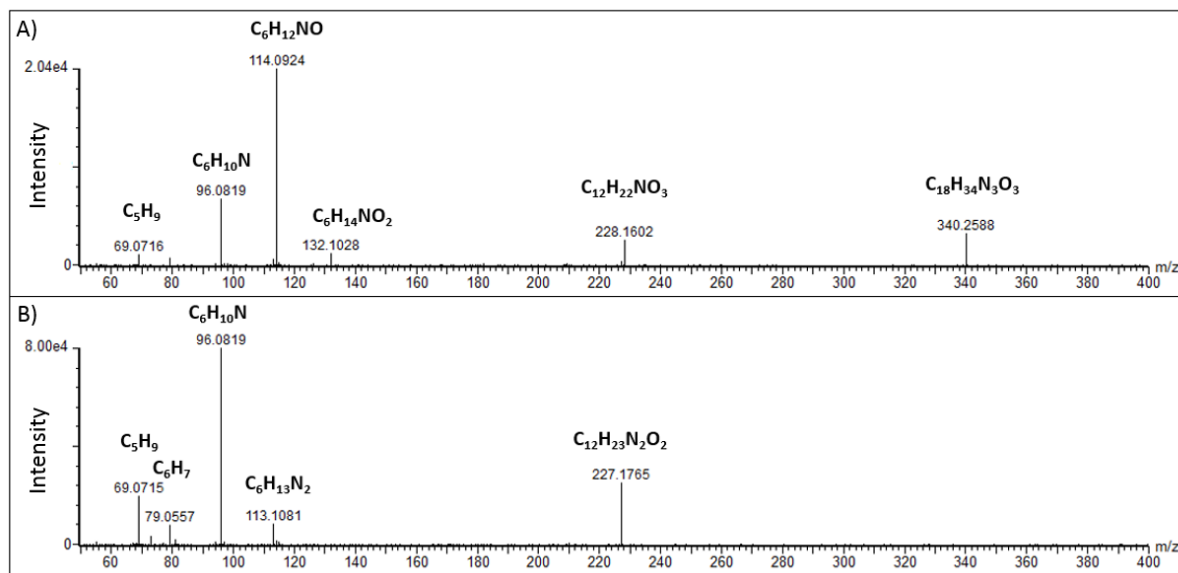
330 **Figure 7:** LC/ESI⁺-MS chromatogram of Milli-Q water, Fisher water and AS (99.5 %) solution of 1.5 M (EXP C1) with corresponding major ion masses associated with raw formulas. The bold ion masses and proposed raw formula were studied in MS-MS (EXP C9). Ions marked with * were detected in their [M-H]⁺ form in LC/ESI-MS (in EXP C6-8).

For further identification and for detection in the negative mode, AS crystals and solutions at various concentrations were extracted using different solvents and different methods (C3-7 in Table 2). In the positive mode, more than 60 % of the molecules identified by direct injection were also detected. Compared to other solvents, acetonitrile was found to be the most efficient extracting solvent. In the negative mode, the signal was systematically much lower (ion current intensity < 10³ counts per second) and only molecules marked as * in Fig. 7 were detected. Consequently, no further analysis was performed in the negative mode due to the low signal. In EXP C8 and C10, another mark of AS crystals of the same purity (99.5 %) was tested for comparison, and revealed that some common ions were detected (in the positive mode) but at a much lower intensity (by a factor of ~ 20), thus demonstrating that the detected organic compounds were present in both AS crystals and that the level of organic contamination depends at least in part on the AS mark. EMSURE® products are supposed to offer a high level of quality and appear to be less contaminated despite the same reported purity. Figure 8 shows the MS-MS measurements operated on two ions detected in EXP C9 (see SI7 for the complete MS-MS results). These results support the proposed raw formula, confirming that these organic compounds contained oxygen and nitrogen and/or sulfur. They also show recurrent fragments: for instance, fragment ion at m/z 96.082, most likely described by the raw formula C₆H₁₀N, was found in all the MS-MS

335
340



345 spectra as well as the fragment ion at m/z 69.072 corresponding to C_5H_9 which was also a fragment observed in the spectra from the HR-ToF-AMS. However, the latter instrument did not detect fragments at $m/z > 100$ due to electron impact ionization that induce high fragmentation.



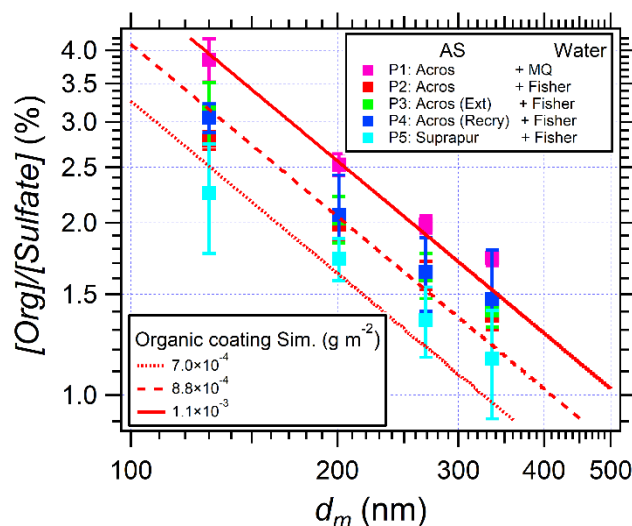
350 **Figure 8:** Mass spectra obtained from LC/ESI⁺-MS-MS measurements of two detected compounds in EXP C9. The [M+H]⁺ ions were detected at : A) m/z 340, using a collision energy of 25 eV; and B) m/z 227, using a collision energy of 20 eV.

355 These results confirm that the organic compounds present in AS are large molecules: out of the 20 most intense detected molecules, 12 contained 12 carbon atoms (C_{12}), and the others contained C_6 (2 molecules bearing $C_xH_yN_{1/2}$), C_{10} (1 molecule), C_{11} (1 molecule), C_{17} (1 molecule), C_{18} (2 molecules) and up to C_{24} (1 molecule), with m/z ranging from 96 to 533. Apart from the 2 smallest molecules (C_6), all of them bear mono- or poly-functional groups with at least 2 heteroatoms (N and O are always present, and S is found in 10 molecules) confirming their low volatility. Most of them fragment following the same scheme, thus showing similar structures. No structure is proposed here as there are many possible structures. The fact that these molecules were largely detected in the positive mode and that they all bear at least one N atom, and the fact that they were observed specifically at the surface of the suspended AS particles, could suggest that they are cationic surfactants such as quaternary ammonium salts remaining from the manufacturing processes. Ammonium sulfate is typically produced by the reaction of gaseous ammonia with sulfuric acid, but the precise manufacturing processes and raw materials of the suppliers are not known in detail and therefore do not allow us to draw any conclusions for these processes.



3.5 Removing organic traces from AS suspended particles

365 To give recommendations on the use of AS for laboratory studies or instrument calibrations with organic contaminations as low as possible, the results of EXP P2 to P5 using high quality water and AS or purified AS crystals, are shown in Figure 9 where $[\text{Org}]/[\text{Sulfate}]$ is plotted versus particle size.



370 **Figure 9 :** $[\text{Org}]/[\text{Sulfate}]$ in AS suspended particles as function of mobility diameter in EXP P1 to P5. The red lines represent the calculated $[\text{Org}]/[\text{Sulfate}]$ simulating surface coating of organic matter (from Eq. 3) for EXP P1, P4 and P5.

Figure 9 shows that, although decreasing with increasing purification, organic traces remain present in all experiments. They seem to remain coated at the surface of the particles, as shown by the good agreement between the simulations and experimental data. According to the simulation results, a reduction of 20 % of $[\text{Org}]/[\text{Sulfate}]$ ratios is observed when Fisher water (red squares) replaces Milli-Q water (pink squares). This reduction might be due to the removing of Nylon polymers found in Milli-Q water (Figure 7). However, no significant difference is observed between EXP P2, P3 and P4, i.e., purification of AS crystals by acetonitrile or recrystallization are not sufficiently efficient to remove organic traces. Finally, comparing EXP P5 (cyan squares) and P2 (red squares), another 20 % reduction of organic traces is observed when highly pure AS crystals were used (99.9999 %). In this case, the organic traces are lower than 2.5 % on the AS particles.

380 4. Conclusions and implications

Ammonium sulfate is one of the dominant components of atmospheric aerosol and is widely used in laboratory experiments and for instrument calibration purposes. However, the widely used commercial AS crystals may contain interfering organic impurities. To answer questions related to the quantity and the quality of organic impurities found in a wide range of commercial AS products, a series of experiments were performed to quantify and identify organic impurities on AS



385 suspended particles and in liquid solutions using a HR-ToF-AMS and a LC-MS. The results showed that, using 99.5 % purity
AS, up to 3.8 % of organic impurities were present related to sulfate mass. This ratio was found to be independent of the
concentration of nebulized AS solutions but was inversely related to the particle size. The simulations of AS-Organic mixtures
showed a homogeneous organic coating on the surface of AS particles with a constant surface density of $1.1 \times 10^{-3} \text{ g.m}^{-2}$.
Regarding to the particle size selection system, the comparison between AAC and DMA showed consistent [Org]/[Sulfate]
390 ratio, thus highlighting that the observed particle size effects were not due to instrumental artifacts. The chemical analysis
of the organic content showed that their structures are independent to the particle size. Up to 20 different molecules have been
detected in AS solutions, and consistent raw formulas were proposed. These formulas include mostly C_{12} compounds with
mono- or poly-functional groups with at least two heteroatoms (N and O were always present, and S was found in 10 molecules)
confirming their low volatility. As these molecules were largely detected in the positive mode by LC-MS, all carrying at least
395 one nitrogen atom. Based on the observation that they are coated at the surface of the suspended AS particles. It can be
suggested that they are cationic surfactants such as quaternary ammonium salts remaining from the manufacturing processes.

The presence of low volatile, probably surface-active organic compounds in commercial AS products is extremely
important for laboratory aerosol studies. In this work, some efforts to remove these organic impurities have been tentatively
tested by purifying and recrystallizing AS crystals. Though no significant difference was observed, it is likely that better results
400 could be obtained by increasing the number of purification and recrystallization cycles, as very high purity AS crystals
(99.9999 %) showed significantly lower organic content. It is therefore recommended to use AS seeds with caution, especially
when small particles are used, in terms of AS purity and water purity when aqueous solutions are used for atomization.

Appendix A: Morphological properties of AS aerosols

Following the method of Zelenyuk et al., (2006), the shape factor (χ) in any flow regime (continuous and transient)
405 can be determined by the ratio of d_{va}/d_m in Eq. A1.

$$\frac{d_{va}}{d_m} = \frac{\rho_p}{\rho_0} \frac{1}{\chi^2} \frac{C_c(d_{va} \chi \rho_p / \rho_0)}{C_c(d_m)} \quad (\text{A1})$$

Where ρ_p is the particle density, ρ_0 is the standard density noticed as 1 g cm^{-3} , C_c is the Cunningham slip factor (Kim et al.,
2005), given by Eq. A2.

$$C_c(K_n) = 1 + K_n \left[1.165 + 0.483 \exp \left(-\frac{0.997}{K_n} \right) \right] \quad (\text{A2})$$

$K_n(d) = 2\lambda_g/d$ is the Knudsen number, and λ_g is the gas mean free path. In this work, normal temperature and pressure
(293.15 K at 1 atm) were applied for the calculation of the shape factor of AS aerosols.

410 The shape factor (χ) of monodisperse AS aerosols selected by the AAC was calculated according to Eq. A1 and is shown in
Table A1, together with the aerodynamic diameter (d_a) selected in the AAC, the mobility diameter d_m and the vacuum
aerodynamic diameter d_{va} representing the average mode of size distributions given by the SMPS and HR-ToF-AMS (p-ToF



mode), respectively. Table A1 shows that, within the uncertainty, the selected AS particles own a size-independent shape factor of 1.06, which falls in the interval of 1.03 and 1.07 reported by (Zelenyuk et al., 2006).

415 Table A1: Morphological properties of monodisperse AS aerosols selected by the AAC (in EXP P1 and P2): aerodynamic diameter (d_a), mobility diameter (d_m), vacuum aerodynamic diameter (d_{va}), and shape factor (χ). The uncertainty represents the standard deviation of several measurements under the same selection condition.

d_a (nm)	d_m (nm)	d_{va} (nm)	Shape factor (χ)
200	126.6 ± 0.3	206 ± 6	1.05 ± 0.02
300	194.3 ± 0.3	312 ± 8	1.06 ± 0.02
400	267.6 ± 0.4	429 ± 10	1.06 ± 0.02
500	340.3 ± 0.4	539 ± 11	1.07 ± 0.02

Author contribution.

420 JW and AM provided the initial idea of this work. JW and BT performed the experiments and data analysis of AS aerosol characterization with the HR-ToF-AMS. NB and SR carried out the measurements of AS solutions with the LC-MS. JW, NB and JC proposed different purification processes of AS aerosols. The organic-inorganic mixing model was provided firstly by JW and improved by BR and AM. JW, NB, JG and AM developed the structure of this paper. JW summarized all contributions and expressed them in this paper. All authors provided advice regarding to the improvement of this paper as well as to the
425 writing of the final manuscript.

Acknowledgements.

The authors acknowledge the support from the French National Research Agency (ANR-PRCI) and the German Research Foundation (DFG) through the project PARAMOUNT (ANR18-CE92-0038-02). The authors also thank the support from the project ORACLE (ANR-20-CE93-0008-01_ACT) from ANR-PRCI.

430 References

Abbatt, J. P. D., Broekhuizen, K., and Pradeep Kumar, P.: Cloud condensation nucleus activity of internally mixed ammonium sulfate/organic acid aerosol particles, *Atmos. Environ.*, 39, 4767–4778, <https://doi.org/10.1016/j.atmosenv.2005.04.029>, 2005.

Aiken, A. C., DeCarlo, P. F., and Jimenez, J. L.: Elemental Analysis of Organic Species with Electron Ionization High-Resolution Mass Spectrometry, *Anal. Chem.*, 79, 8350–8358, <https://doi.org/10.1021/ac071150w>, 2007.

435 Andreae, M. O. and Rosenfeld, D.: Aerosol–cloud–precipitation interactions. Part 1. The nature and sources of cloud-active aerosols, *Earth-Sci. Rev.*, 89, 13–41, <https://doi.org/10.1016/j.earscirev.2008.03.001>, 2008.



- Badger, C. L., George, I., Griffiths, P. T., Braban, C. F., Cox, R. A., and Abbatt, J. P. D.: Phase transitions and hygroscopic growth of aerosol particles containing humic acid and mixtures of humic acid and ammonium sulphate, *Atmospheric Chem. Phys.*, 6, 755–768, <https://doi.org/10.5194/acp-6-755-2006>, 2006.
- 440 Brooks, S. D., DeMott, P. J., and Kreidenweis, S. M.: Water uptake by particles containing humic materials and mixtures of humic materials with ammonium sulfate, *Atmos. Environ.*, 38, 1859–1868, <https://doi.org/10.1016/j.atmosenv.2004.01.009>, 2004.
- Canagaratna, M. R., Jimenez, J. L., Kroll, J. H., Chen, Q., Kessler, S. H., Massoli, P., Hildebrandt Ruiz, L., Fortner, E., Williams, L. R., Wilson, K. R., Surratt, J. D., Donahue, N. M., Jayne, J. T., and Worsnop, D. R.: Elemental ratio measurements
445 of organic compounds using aerosol mass spectrometry: characterization, improved calibration, and implications, *Atmospheric Chem. Phys.*, 15, 253–272, <https://doi.org/10.5194/acp-15-253-2015>, 2015.
- Charlson, R. J., Schwartz, S., Hales, J., Cess, R. D., Coakley, J. J., Hansen, J., and Hofmann, D.: Climate forcing by anthropogenic aerosols, *Science*, 255, 423–430, 1992.
- Clegg, S. L., Brimblecombe, P., and Wexler, A. S.: Thermodynamic Model of the System $\text{H}^+ - \text{NH}_4^+ - \text{Na}^+ - \text{SO}_4^{2-} - \text{NO}_3^- - \text{Cl}^- - \text{H}_2\text{O}$ at 298.15 K, *J. Phys. Chem. A*, 102, 2155–2171, <https://doi.org/10.1021/jp973043j>, 1998.
- 450 Darer, A. I., Cole-Filipiak, N. C., O'Connor, A. E., and Elrod, M. J.: Formation and stability of atmospherically relevant isoprene-derived organosulfates and organonitrates, *Environ. Sci. Technol.*, 45, 1895–1902, 2011.
- De Haan, D. O., Hawkins, L. N., Welsh, H. G., Pednekar, R., Casar, J. R., Pennington, E. A., de Loera, A., Jimenez, N. G., Symons, M. A., Zauscher, M., Pajunoja, A., Caponi, L., Cazaunau, M., Formenti, P., Gratien, A., Pangui, E., and Doussin, J.-
455 F.: Brown Carbon Production in Ammonium- or Amine-Containing Aerosol Particles by Reactive Uptake of Methylglyoxal and Photolytic Cloud Cycling, *Environ. Sci. Technol.*, 51, 7458–7466, <https://doi.org/10.1021/acs.est.7b00159>, 2017.
- DeCarlo, P. F., Slowik, J. G., Worsnop, D. R., Davidovits, P., and Jimenez, J. L.: Particle Morphology and Density Characterization by Combined Mobility and Aerodynamic Diameter Measurements. Part 1: Theory, *Aerosol Sci. Technol.*, 38, 1185–1205, <https://doi.org/10.1080/027868290903907>, 2004.
- 460 DeCarlo, P. F., Kimmel, J. R., Trimborn, A., Northway, M. J., Jayne, J. T., Aiken, A. C., Gonin, M., Fuhrer, K., Horvath, T., Docherty, K. S., Worsnop, D. R., and Jimenez, J. L.: Field-Deployable, High-Resolution, Time-of-Flight Aerosol Mass Spectrometer, *Anal. Chem.*, 78, 8281–8289, <https://doi.org/10.1021/ac061249n>, 2006.
- Engelhart, G. J., Asa-Awuku, A., Nenes, A., and Pandis, S. N.: CCN activity and droplet growth kinetics of fresh and aged monoterpene secondary organic aerosol, *Atmospheric Chem. Phys.*, 8, 3937–3949, <https://doi.org/10.5194/acp-8-3937-2008>,
465 2008.
- Gérard, V., Nozière, B., Fine, L., Ferronato, C., Singh, D. K., Frossard, A. A., Cohen, R. C., Asmi, E., Lihavainen, H., Kivekäs, N., Aurela, M., Brus, D., Frka, S., and Cvitešić Kušan, A.: Concentrations and Adsorption Isotherms for Amphiphilic Surfactants in PM₁ Aerosols from Different Regions of Europe, *Environ. Sci. Technol.*, 53, 12379–12388, <https://doi.org/10.1021/acs.est.9b03386>, 2019.



- 470 Grace, D. N., Lugos, E. N., Ma, S., Griffith, D. R., Hendrickson, H. P., Woo, J. L., and Galloway, M. M.: Brown Carbon Formation Potential of the Biacetyl–Ammonium Sulfate Reaction System, *ACS Earth Space Chem.*, 4, 1104–1113, <https://doi.org/10.1021/acsearthspacechem.0c00096>, 2020.
- Hämeri, K., Charlson, R., and Hansson, H.-C.: Hygroscopic properties of mixed ammonium sulfate and carboxylic acids particles, *AIChE J.*, 48, 1309–1316, <https://doi.org/10.1002/aic.690480617>, 2002.
- 475 Hawkins, L. N., Welsh, H. G., and Alexander, M. V.: Evidence for pyrazine-based chromophores in cloud water mimics containing methylglyoxal and ammonium sulfate, *Atmospheric Chem. Phys.*, 18, 12413–12431, <https://doi.org/10.5194/acp-18-12413-2018>, 2018.
- Hensley, J. C., Birdsall, A. W., Valtierra, G., Cox, J. L., and Keutsch, F. N.: Revisiting the reaction of dicarbonyls in aerosol proxy solutions containing ammonia: the case of butenedial, *Atmospheric Chem. Phys.*, 21, 8809–8821, <https://doi.org/10.5194/acp-21-8809-2021>, 2021.
- 480 IPCC: Climate Change 2013 – The Physical Science Basis: Working Group I Contribution to the Fifth Assessment Report of the Intergovernmental Panel on Climate Change, Cambridge University Press, Cambridge, <https://doi.org/10.1017/CBO9781107415324>, 2013.
- Jimenez, J. L., Canagaratna, M. R., Donahue, N. M., Prevot, A. S. H., Zhang, Q., Kroll, J. H., DeCarlo, P. F., Allan, J. D., Coe, H., Ng, N. L., Aiken, A. C., Docherty, K. S., Ulbrich, I. M., Grieshop, A. P., Robinson, A. L., Duplissy, J., Smith, J. D., Wilson, K. R., Lanz, V. A., Hueglin, C., Sun, Y. L., Tian, J., Laaksonen, A., Raatikainen, T., Rautiainen, J., Vaattovaara, P., Ehn, M., Kulmala, M., Tomlinson, J. M., Collins, D. R., Cubison, M. J., E, Dunlea, J., Huffman, J. A., Onasch, T. B., Alfarra, M. R., Williams, P. I., Bower, K., Kondo, Y., Schneider, J., Drewnick, F., Borrmann, S., Weimer, S., Demerjian, K., Salcedo, D., Cottrell, L., Griffin, R., Takami, A., Miyoshi, T., Hatakeyama, S., Shimojo, A., Sun, J. Y., Zhang, Y. M., Dzepina, K., Kimmel, J. R., Sueper, D., Jayne, J. T., Herndon, S. C., Trimborn, A. M., Williams, L. R., Wood, E. C., Middlebrook, A. M., Kolb, C. E., Baltensperger, U., and Worsnop, D. R.: Evolution of Organic Aerosols in the Atmosphere, *Science*, 326, 1525–1529, <https://doi.org/10.1126/science.1180353>, 2009.
- 490 Johnson, T. J., Irwin, M., Symonds, J. P. R., Olfert, J. S., and Boies, A. M.: Measuring aerosol size distributions with the aerodynamic aerosol classifier, *Aerosol Sci. Technol.*, 52, 655–665, <https://doi.org/10.1080/02786826.2018.1440063>, 2018.
- 495 Kampf, C. J., Jakob, R., and Hoffmann, T.: Identification and characterization of aging products in the glyoxal/ammonium sulfate system – implications for light-absorbing material in atmospheric aerosols, *Atmospheric Chem. Phys.*, 12, 6323–6333, <https://doi.org/10.5194/acp-12-6323-2012>, 2012.
- Keller, B. O., Sui, J., Young, A. B., and Whittall, R. M.: Interferences and contaminants encountered in modern mass spectrometry, *Anal. Chim. Acta*, 627, 71–81, <https://doi.org/10.1016/j.aca.2008.04.043>, 2008.
- 500 Kim, J. H., Mulholland, G. W., Kukuck, S. R., and Pui, D. Y. H.: Slip Correction Measurements of Certified PSL Nanoparticles Using a Nanometer Differential Mobility Analyzer (Nano-DMA) for Knudsen Number From 0.5 to 83, *J. Res. Natl. Inst. Stand. Technol.*, 110, 31–54, <https://doi.org/10.6028/jres.110.005>, 2005.



- Kind, T. and Fiehn, O.: Seven Golden Rules for heuristic filtering of molecular formulas obtained by accurate mass spectrometry, *BMC Bioinformatics*, 8, 105, <https://doi.org/10.1186/1471-2105-8-105>, 2007.
- 505 King, S. M., Rosenoern, T., Shilling, J. E., Chen, Q., and Martin, S. T.: Increased cloud activation potential of secondary organic aerosol for atmospheric mass loadings, *Atmospheric Chem. Phys.*, 9, 2959–2971, <https://doi.org/10.5194/acp-9-2959-2009>, 2009.
- Koehler, K. A., Kreidenweis, S. M., DeMott, P. J., Prenni, A. J., Carrico, C. M., Ervens, B., and Feingold, G.: Water activity and activation diameters from hygroscopicity data - Part II: Application to organic species, *Atmospheric Chem. Phys.*, 6, 795–
- 510 809, <https://doi.org/10.5194/acp-6-795-2006>, 2006.
- Laskin, J., Laskin, A., Nizkorodov, S. A., Roach, P., Eckert, P., Gilles, M. K., Wang, B., Lee, H. J. (Julie), and Hu, Q.: Molecular Selectivity of Brown Carbon Chromophores, *Environ. Sci. Technol.*, 48, 12047–12055, <https://doi.org/10.1021/es503432r>, 2014.
- Liggio, J., Li, S.-M., and McLaren, R.: Heterogeneous Reactions of Glyoxal on Particulate Matter: Identification of Acetals
- 515 and Sulfate Esters, *Environ. Sci. Technol.*, 39, 1532–1541, <https://doi.org/10.1021/es048375y>, 2005.
- Meyer, N. K., Duplissy, J., Gysel, M., Metzger, A., Dommen, J., Weingartner, E., Alfarra, M. R., Prevot, A. S. H., Fletcher, C., Good, N., McFiggans, G., Jonsson, Å. M., Hallquist, M., Baltensperger, U., and Ristovski, Z. D.: Analysis of the hygroscopic and volatile properties of ammonium sulphate seeded and unseeded SOA particles, *Atmospheric Chem. Phys.*, 9, 721–732, <https://doi.org/10.5194/acp-9-721-2009>, 2009.
- 520 Moore, R. H., Ingall, E. D., Sorooshian, A., and Nenes, A.: Molar mass, surface tension, and droplet growth kinetics of marine organics from measurements of CCN activity, *Geophys. Res. Lett.*, 35, <https://doi.org/10.1029/2008GL033350>, 2008.
- Nandy, L. and Dutcher, C. S.: Phase Behavior of Ammonium Sulfate with Organic Acid Solutions in Aqueous Aerosol Mimics Using Microfluidic Traps, *J. Phys. Chem. B*, 122, 3480–3490, <https://doi.org/10.1021/acs.jpcc.7b10655>, 2018.
- Nozière, B., Baduel, C., and Jaffrezo, J.-L.: The dynamic surface tension of atmospheric aerosol surfactants reveals new aspects
- 525 of cloud activation, *Nat. Commun.*, 5, 3335, <https://doi.org/10.1038/ncomms4335>, 2014.
- Ovadnevaite, J., Zuend, A., Laaksonen, A., Sanchez, K. J., Roberts, G., Ceburnis, D., Decesari, S., Rinaldi, M., Hodas, N., Facchini, M. C., Seinfeld, J. H., and O’ Dowd, C.: Surface tension prevails over solute effect in organic-influenced cloud droplet activation, *Nature*, 546, 637–641, <https://doi.org/10.1038/nature22806>, 2017.
- Petters, M. D.: A language to simplify computation of differential mobility analyzer response functions, *Aerosol Sci. Technol.*,
- 530 52, 1437–1451, <https://doi.org/10.1080/02786826.2018.1530724>, 2018.
- Petters, M. D. and Kreidenweis, S. M.: A single parameter representation of hygroscopic growth and cloud condensation nucleus activity, *Atmospheric Chem. Phys.*, 7, 1961–1971, <https://doi.org/10.5194/acp-7-1961-2007>, 2007.
- Petters, M. D. and Kreidenweis, S. M.: A single parameter representation of hygroscopic growth and cloud condensation nucleus activity – Part 3: Including surfactant partitioning, *Atmospheric Chem. Phys.*, 13, 1081–1091,
- 535 <https://doi.org/10.5194/acp-13-1081-2013>, 2013.



- Pöschl, U. and Shiraiwa, M.: Multiphase Chemistry at the Atmosphere–Biosphere Interface Influencing Climate and Public Health in the Anthropocene, *Chem. Rev.*, 115, 4440–4475, <https://doi.org/10.1021/cr500487s>, 2015.
- Powelson, M. H., Espelien, B. M., Hawkins, L. N., Galloway, M. M., and De Haan, D. O.: Brown Carbon Formation by Aqueous-Phase Carbonyl Compound Reactions with Amines and Ammonium Sulfate, *Environ. Sci. Technol.*, 48, 985–993, <https://doi.org/10.1021/es4038325>, 2014.
- 540 Prenni, A. J., DeMott, P. J., and Kreidenweis, S. M.: Water uptake of internally mixed particles containing ammonium sulfate and dicarboxylic acids, *Atmos. Environ.*, 37, 4243–4251, [https://doi.org/10.1016/S1352-2310\(03\)00559-4](https://doi.org/10.1016/S1352-2310(03)00559-4), 2003.
- Saukko, E., Zorn, S., Kuwata, M., Keskinen, J., and Virtanen, A.: Phase State and Deliquescence Hysteresis of Ammonium-Sulfate-Seeded Secondary Organic Aerosol, *Aerosol Sci. Technol.*, 49, 531–537, <https://doi.org/10.1080/02786826.2015.1050085>, 2015.
- 545 Seinfeld, J. H., Bretherton, C., Carslaw, K. S., Coe, H., DeMott, P. J., Dunlea, E. J., Feingold, G., Ghan, S., Guenther, A. B., Kahn, R., Kraucunas, I., Kreidenweis, S. M., Molina, M. J., Nenes, A., Penner, J. E., Prather, K. A., Ramanathan, V., Ramaswamy, V., Rasch, P. J., Ravishankara, A. R., Rosenfeld, D., Stephens, G., and Wood, R.: Improving our fundamental understanding of the role of aerosol–cloud interactions in the climate system, *Proc. Natl. Acad. Sci.*, 113, 5781–5790, <https://doi.org/10.1073/pnas.1514043113>, 2016.
- 550 Sjogren, S., Gysel, M., Weingartner, E., Baltensperger, U., Cubison, M. J., Coe, H., Zardini, A. A., Marcolli, C., Krieger, U. K., and Peter, T.: Hygroscopic growth and water uptake kinetics of two-phase aerosol particles consisting of ammonium sulfate, adipic and humic acid mixtures, *J. Aerosol Sci.*, 38, 157–171, <https://doi.org/10.1016/j.jaerosci.2006.11.005>, 2007.
- Smith, M. L., You, Y., Kuwata, M., Bertram, A. K., and Martin, S. T.: Phase Transitions and Phase Miscibility of Mixed Particles of Ammonium Sulfate, Toluene-Derived Secondary Organic Material, and Water, *J. Phys. Chem. A*, 117, 8895–8906, <https://doi.org/10.1021/jp405095e>, 2013.
- 555 Sorjamaa, R., Svenningsson, B., Raatikainen, T., Henning, S., Bilde, M., and Laaksonen, A.: The role of surfactants in Köhler theory reconsidered, *Atmospheric Chem. Phys.*, 4, 2107–2117, <https://doi.org/10.5194/acp-4-2107-2004>, 2004.
- Stokes, R. H. and Robinson, R. A.: Interactions in Aqueous Nonelectrolyte Solutions. I. Solute-Solvent Equilibria, *J. Phys. Chem.*, 70, 2126–2131, <https://doi.org/10.1021/j100879a010>, 1966.
- 560 Surratt, J. D., Gómez-González, Y., Chan, A. W. H., Vermeylen, R., Shahgholi, M., Kleindienst, T. E., Edney, E. O., Offenberg, J. H., Lewandowski, M., Jaoui, M., Maenhaut, W., Claeys, M., Flagan, R. C., and Seinfeld, J. H.: Organosulfate Formation in Biogenic Secondary Organic Aerosol, *J. Phys. Chem. A*, 112, 8345–8378, <https://doi.org/10.1021/jp802310p>, 2008.
- 565 Tavakoli, F. and Olfert, J. S.: An Instrument for the Classification of Aerosols by Particle Relaxation Time: Theoretical Models of the Aerodynamic Aerosol Classifier, *Aerosol Sci. Technol.*, 47, 916–926, <https://doi.org/10.1080/02786826.2013.802761>, 2013.



- 570 Tervahattu, H., Hartonen, K., Kerminen, V.-M., Kupiainen, K., Aarnio, P., Koskentalo, T., Tuck, A. F., and Vaida, V.: New evidence of an organic layer on marine aerosols, *J. Geophys. Res. Atmospheres*, 107, AAC 1-1-AAC 1-8, <https://doi.org/10.1029/2000JD000282>, 2002.
- Trainic, M., Abo Rziq, A., Lavi, A., Flores, J. M., and Rudich, Y.: The optical, physical and chemical properties of the products of glyoxal uptake on ammonium sulfate seed aerosols, *Atmospheric Chem. Phys.*, 11, 9697–9707, <https://doi.org/10.5194/acp-11-9697-2011>, 2011.
- 575 Tran, J. C. and Doucette, A. A.: Cyclic polyamide oligomers extracted from nylon 66 membrane filter disks as a source of contamination in liquid chromatography/mass spectrometry, *J. Am. Soc. Mass Spectrom.*, 17, 652–656, <https://doi.org/10.1016/j.jasms.2006.01.008>, 2006.
- Treuel, L., Pederzani, S., and Zellner, R.: Deliquescence behaviour and crystallisation of ternary ammonium sulfate/dicarboxylic acid/water aerosols, *Phys. Chem. Chem. Phys.*, 11, 7976–7984, <https://doi.org/10.1039/B905007H>, 2009.
- 580 Varutbangkul, V., Brechtel, F. J., Bahreini, R., Ng, N. L., Keywood, M. D., Kroll, J. H., Flagan, R. C., Seinfeld, J. H., Lee, A., and Goldstein, A. H.: Hygroscopicity of secondary organic aerosols formed by oxidation of cycloalkenes, monoterpenes, sesquiterpenes, and related compounds, *Atmospheric Chem. Phys.*, 6, 2367–2388, <https://doi.org/10.5194/acp-6-2367-2006>, 2006.
- Wex, H., Petters, M. D., Carrico, C. M., Hallbauer, E., Massling, A., McMeeking, G. R., Poulain, L., Wu, Z., Kreidenweis, S. M., and Stratmann, F.: Towards closing the gap between hygroscopic growth and activation for secondary organic aerosol: 585 Part 1 – Evidence from measurements, *Atmospheric Chem. Phys.*, 9, 3987–3997, <https://doi.org/10.5194/acp-9-3987-2009>, 2009.
- Wiedensohler, A., Birmili, W., Nowak, A., Sonntag, A., Weinhold, K., Merkel, M., Wehner, B., Tuch, T., Pfeifer, S., Fiebig, M., Fjåraa, A. M., Asmi, E., Sellegri, K., Depuy, R., Venzac, H., Villani, P., Laj, P., Aalto, P., Ogren, J. A., Swietlicki, E., Williams, P., Roldin, P., Quincey, P., Hüglin, C., Fierz-Schmidhauser, R., Gysel, M., Weingartner, E., Riccobono, F., Santos, 590 S., Grüning, C., Faloon, K., Beddows, D., Harrison, R., Monahan, C., Jennings, S. G., O’Dowd, C. D., Marinoni, A., Horn, H.-G., Keck, L., Jiang, J., Scheckman, J., McMurry, P. H., Deng, Z., Zhao, C. S., Moerman, M., Henzing, B., de Leeuw, G., Löschau, G., and Bastian, S.: Mobility particle size spectrometers: harmonization of technical standards and data structure to facilitate high quality long-term observations of atmospheric particle number size distributions, *Atmospheric Meas. Tech.*, 5, 657–685, <https://doi.org/10.5194/amt-5-657-2012>, 2012.
- 595 Zelenyuk, A., Cai, Y., and Imre, D.: From Agglomerates of Spheres to Irregularly Shaped Particles: Determination of Dynamic Shape Factors from Measurements of Mobility and Vacuum Aerodynamic Diameters, *Aerosol Sci. Technol.*, 40, 197–217, <https://doi.org/10.1080/02786820500529406>, 2006.